Chemical Engineering Journal 287 (2016) 474–481

Contents lists available at ScienceDirect

Chemical Engineering Journal

journal homepage: www.elsevier.com/locate/cej

Electrospun fibrous membrane with enhanced swithchable oil/water wettability for oily water separation

Jin-Jin Li, Li-Tao Zhu, Zheng-Hong Luo *

Department of Chemical Engineering, School of Chemistry and Chemical Engineering, Shanghai Jiao Tong University, Shanghai 200240, PR China

HIGHLIGHTS

- Both solution-casting and electrospinning methods are used to fabricate smart membranes.
- Electrospun fibrous membrane owns an extended transition range of oil/water wettability.
- The as-prepared membranes realize many types oil/water separations through regulating the temperature.
- The separations are driven only by gravity and exhibit excellent efficiency higher than 98.5%.
- Electrospun fibrous membrane achieves a higher liquid flux due to the high porosity and the large surface-to-volume ratio.

GRAPHICAL ABSTRACT

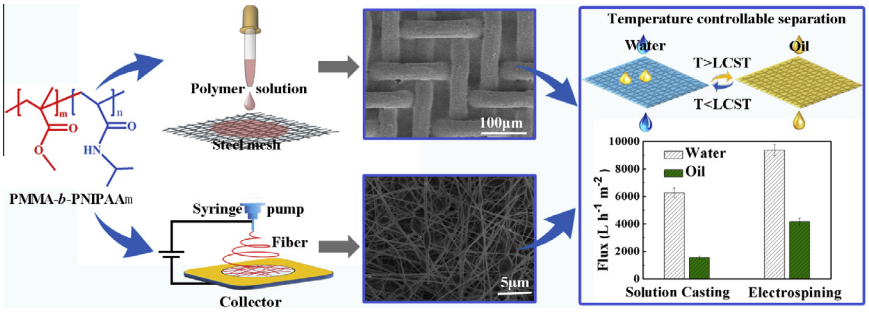

ARTICLE INFO

Article history:
Received 14 October 2015
Received in revised form 12 November 2015
Accepted 14 November 2015
Available online 23 November 2015

Keywords:
Solution-casting membrane
Electrospun fibrous membrane
Smart surface
Wettability
Oil/water separation

ABSTRACT

Smart polymeric surfaces with switchable oil/water wettability are ideal candidates for oil/water separation, which still suffer from significant restrictions in practical separation applications. Appropriate fabrication method should be explored to devise and mass produce smart polymeric membranes. Herein, we prepared two smart membranes through solution-casting method and electrospinning technology, respectively, based on temperature-responsive copolymer poly(methyl methacrylate)-block-poly(N-iso propylacrylamide) (PMMA-*b*-PNIPAAm). According to the thermo-responsive component PNIPAAm, both membranes exhibited temperature-modulable oil/water wettability. Electrospun fibrous membrane owned an extended transition range of oil/water wettability compared to polymer solution-casting membrane because of its 3D network porous structure of the random entangled fibers. The as-prepared membranes realized gravity-driven oil/water separation with efficiency higher than 98% through regulating temperature. Solution-casting membrane exhibited a water flux of about 6200 L h^{-1} m^{-2} and an oil flux of about 1550 L h^{-1} m^{-2}. By contrast, characteristics of the high porosity and the large surface-to-volume ratio made the electrospun fibrous membrane achieve higher fluxes of about 9400 L h^{-1} m^{-2} for water and about 4200 L h^{-1} for oil. Electrospinning is a powerful and cost-effective method to construct smart membrane with excellent wetting property and separation performance.

1. Introduction

The discharge of oily wastewater generated by humankind's production and frequent oil spill accidents damages the

* Corresponding author. Tel./fax: +86 21 54745602.
E-mail address: luozh@sjtu.edu.cn (Z.-H. Luo).

http://dx.doi.org/10.1016/j.cej.2015.11.057
1385-8947/

environment and threatens biological and human safety. Efficient technologies to handle the oil contaminated wastewater are highly desired yet still challenging [1,2]. Recently, smart interfaces have received intense attentions in the application for oily waste water treatment due to their stimuli-responsive wettability toward oil or water [3]. Responsive polymers, which can reversibly switch their chemical and physical properties in response to stimuli (e.g., pH, temperature, light, electricity and so on), have become one of the most promising materials to construct smart surfaces [4–8]. Until now, some responsive polymer-based smart surfaces have been applied for demanded oil/water separation. For example, Zhang et al. fabricated smart surfaces with switchable wettability through grafting a pH-responsive copolymer of poly(2-vinylpyridine) and polydimethylsiloxane onto textiles and sponges [4]. The as-prepared materials realized the controllable water/oil separation by adjusting the pH of surroundings. Xue and coworkers presented a temperature controlled dual water/oil on–off switch by direct casting of the PMMA-*b*-PNIPAAm copolymer solution onto a common industrial steel mesh [5]. Cao et al. reported a thermo and pH dual-responsive membrane through coating the steel mesh with poly(2-(dimethylamino) ethyl methacrylate) (PDMAEMA) [6]. Depending on the dual-responsive characteristic, the modified mesh can separately collect oil and water by regulating temperature or pH.

Despite of these progresses, smart polymeric surfaces still suffer from significant restriction in practical separation applications. For example, the complex and costly fabrication process, the limited transition range of surface wettability, the inevitable oil fouling, and so on [9,10]. From these perspectives, devising and mass producing functional polymeric surfaces, which possess stimulus- and well-controlled super-wettability toward oil or water, still remain a challenge. Various methods have been used to fabricate smart polymeric surfaces, which include coating process [11,12], surface-initiated polymerization [13], electrospinning [14], self-assembly layer-by-layer [15], and so on. Among them, coating process and electrospinning are relatively simple and low cost, and therefore suitable for practical application. In particular, electrospun fibrous membranes consisting of continuous entangled fibers usually have three-dimensional (3D) network porous structure, which can influence the surface wettability together with the chemical composition. Meanwhile, their high surface area-to-volume ratio makes them act as good candidates for separation applications [16,17].

Herein, to explore the advantage of smart electrospun fibrous membrane in terms of stimulus-responsive transition range of oil/water wettability and separation performance, we prepared two smart membranes through solution-casting method and electrospinning technology, respectively, based on temperature-responsive copolymer poly(methyl methacrylate)-block-poly(N-isopropylacrylamide) (PMMA-*b*-PNIPAAm). PNIPAAm as a comprehensively studied thermo-responsive polymer endowed the as-prepared membranes with temperature switchable wettability. The combination of water-insoluble PMMA can effectively improve the stability of the membranes, and thus largely extend their application scope. However, the oil/water wettability transition range of the membranes responding to temperature is also affected by the surface morphology. Therefore, the surface morphology and the temperature switchable wettability of the as-prepared membranes were systematically investigated. At last, we applied the as-prepared membranes for temperature controlled oil/water separation. The relevant separation mechanism and the different separation performances of the two membranes were further studied.

2. Experimental section

2.1. Materials

The stainless steel mesh with pore size of about 45 μm was purchased from local market. Chloroform, tetrahydrofuran (THF), dimethyl formamide (DMF) were obtained from Sinopharm Chemical Reagent Co., Ltd. (SCRC) and dried prior to be used. Temperature-responsive block copolymer PMMA-*b*-PNIPAAm was synthesized by sequential copper(0)-mediated reversible-deactivation radical polymerization (Cu(0)-mediated RDRP), which has advantages in moderate polymerization condition and perfect end-functionality [18,19]. The sufficient experimental details could be found in our previous work [20]. The macroinitiator, bromine end-capped PMMA (PMMA-Br), was synthesized. Subsequently, PMMA-*b*-PNIPAAm was prepared *via* chain extension of PMMA-Br. The number-average molecular weight (M_n) of PMMA-Br is 15,600 g/mol, and PMMA-*b*-PNIPAAm is 35,900 g/mol. The low polydispersity of the $PMMA_{147}$-Br (M_w/M_n = 1.19) and $PMMA_{147}$-*b*-$PNIPAAm_{178}$ (M_w/M_n = 1.28) demonstrated the well controllability and "living" feature of Cu(0)-mediated RDRP. The volume fraction of PNIPAAm is 0.51, which was calculated according to the known density of PMMA (1.18 g/cm^3) and PNIPAAm (1.39 g/cm^3) [21,22].

2.2. Preparation of copolymers membranes

The purchased stainless steel mesh was treated ultrasonically using acetone and ethyl alcohol in tandem for 30 min, and followed by drying with nitrogen flow. Then the rinsed stainless steel mesh was cut into round shape with area of 2.37×10^{-3} m^2 and used as the substrate for the following smart membrane preparation.

PMMA-*b*-PNIPAAm solution-casting membrane was prepared as follows: 200 mg PMMA-*b*-PNIPAAm was first dissolved in 2 mL chloroform and stirred for 24 h. The precursor solution was cast onto a stainless steel mesh drop by drop. As the solvent evaporated at 50 °C for 12 h, the block copolymer formed a thin layer around the steel wires.

PMMA-*b*-PNIPAAm fibrous membrane was prepared through electrospinning. The typical preparation process was as follows: PMMA-*b*-PNIPAAm was first dissolved in a mixture solvent of DMF/chloroform at a volume ratio of 1/2 to a concentration of 25 wt%. After stirring for 24 h, the prepared solution was electrospun in a closed chamber. During electrospinning, the applied voltage was kept at approximately 14 kV and the solution feeding rate was set at 0.2 mL/h through syringe pump. The as-spun fibers were collected by a pre-cleaned round stainless steel mesh and the obtained fibrous membrane was dried at 50 °C for 12 h to remove any residual solvent.

2.3. Characterization

The morphologies of the as-prepared membranes were obtained by a JEOL JSM-7500F scanning electron microscope (SEM). The contact angles (CA) of as-prepared membranes at different temperatures were measured on a Contact Angle Measuring Instrument (KRUSS, DSA30). The temperature was controlled by a TC40-MK2 temperature controller.

2.4. Separation performance assessment

200 mL layered mixture of oil and water at a volume ratio of 1/1 was poured into the separation device. The flux of liquid (J_w, L m^2 h^{-1}) was obtained by calculating the permeation volume per unit time from the valid area, which was defined as Eq. (1):

$$J_W = \frac{V}{A\Delta t} \quad (1)$$

where, V (L) was the volume of permeated liquid (water or oil), A (m^2) was the valid area for separation and Δt (h) was the permeation time.

3. Results and discussion

3.1. Characterization of smart membranes

Semi-permeable stainless steel mesh possessing mechanical stability has frequently been used as a good substrate for the fabrication of separation membranes [3,10]. Therefore, we deposited temperature-responsive copolymer PMMA-*b*-PNIPAAm on the meshes through solution-casting method and electrospinning technology, respectively, to prepare two smart membranes with completely different surface structures. The fabrication processes were described in Figs. 1a and 2a, respectively. SEM observation results in Figs. 1 and 2 show the morphologies of the meshes before and after modification.

As shown in Fig. 1b, the connected metal wires of the initial mesh are clearly visible and the average size of the square-shaped pores is about 45 μm (350 mesh size). The highly magnified image in Fig. 1c reveals that the surface of the metal wires is smooth. After solution-casting, the mesh is covered with a dense of copolymer film uniformly, but the connected metal wires are still visible as illustrated in Fig. 1d. Furthermore, honeycomb rough surface caused by the rapid evaporation of the solvent is clearly observed on the enlarged view of polymer coated metal wire (Fig. 1e).

As to the electrospun fibrous membrane, the mesh is covered with a dense layer of randomly intertwined fibers with bead and beads-on-string structures shown in Fig. 2b. The highly magnified image in Fig. 2c reveals that the fiber has a smooth surface with an average diameter about 250 nm. Three-dimensional microporous structures formed by the entanglement fibers will improve the liquid permeation rate across the membrane.

3.2. Temperature-responsive wettability of smart membranes

PNIPAAm is a comprehensively studied thermo-responsive polymer with lower critical solution temperature (LCST) of about 32–33 °C. PNIPAAm modified surfaces can reversibly switch between hydrophilicity and hydrophobicity when the temperature fluctuates below and above its LCST [23,24]. Water-insoluble PMMA with high glass transition temperature (T_g) can served as the physical cross-link of hydrophilic PNIPAAm in moist environments. Therefore, the combination of PMMA can effectively improve the stability of the membranes. On the other hand, surface morphology is another important factor that has significant influence on the surface wettability together with the chemical composition [25,26]. To probe the special wettability of the as-prepared membranes obtained by two different fabrication processes, CA measurements on the membrane surfaces were conducted in air and under water at temperature above and below the LCST of PNIPAAm.

Fig. 3 shows the temperature switchable water and oil wetting behaviors of the solution-casting membrane. As shown in Fig. 3-a and b, when the temperature is below the LCST of PNIPAAm at 15 °C, water droplet spreads over the membrane gradually within 80 s in air, indicating the superhydrophilicity of the membrane. On the contrary, hexane droplet forms a sphere with an oil contact angle (OCA) of about 142° on the surface of the membrane underwater in Fig. 3c, showing highly oleophobic property. On the other hand, when the temperature is above the LCST of PNIPAAm at 50 °C, the wettability of the membrane experiences a transition from superhydrophilicity/oleophobicity to hydrophobicity/oleophilicity. A spherical water droplet stably sits on the membrane with a water contact angle (WCA) of about 110° in air (Fig. 3d). The hexane droplet has an OCA of about 55° on the surface in aqueous solution (Fig. 3e). The initial wettability of the membrane recovers upon cooling. The switchable wettability between superhydrophilicity/oleophobicity and hydrophobicity/oleophilicity can be recycled many times with slight fluctuation in responsivity as presented in Fig. 3f.

The switchable surface wettability, relating to the conformation transition of PNIPAAm and the cooperation between PNIPAAm and PMMA, has been confirmed in our previous work [20]. Specifically, at a temperature below the LCST, intermolecular hydrogen bonding interaction between C═O, N—H groups and water makes the PNIPAAm chains become hydrated and swollen. The extended PNIPAAm chains with sufficient mobility expose themselves on the exterior of the surface, featuring the membrane with hydrophilicity. PMMA with a high T_g serves as the stabilizer of hydrophilic amorphous PNIPAAm. The hydrophilic surface, favoring for water

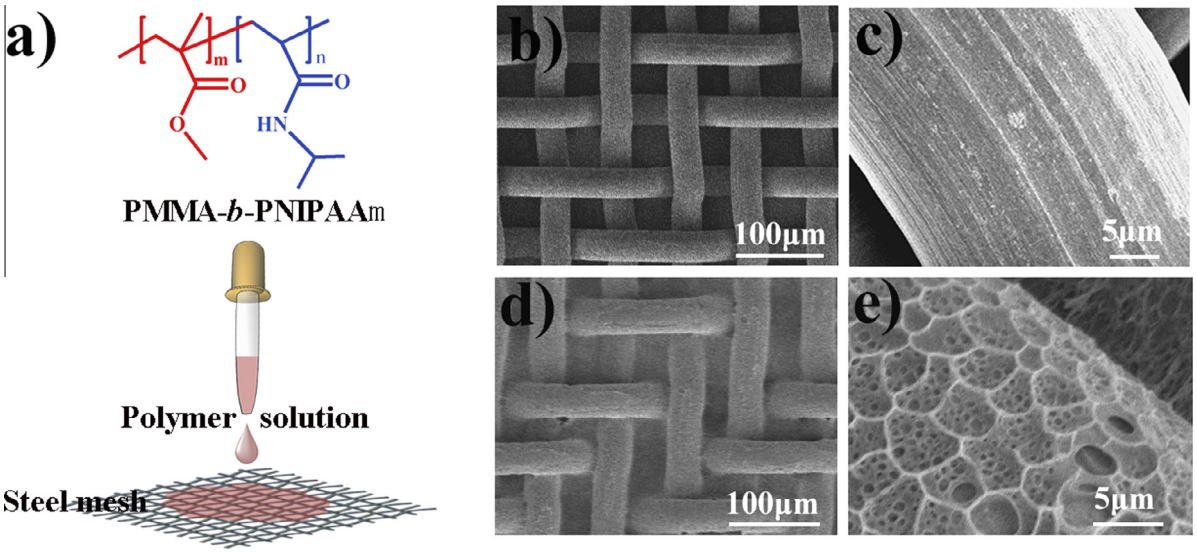

Fig. 1. (a) Diagram of the preparation process for solution-casting membrane. (b and c) SEM images of the initial stainless steel mesh with different magnifications. (d and e) SEM images of solution-casting membrane with different magnifications.

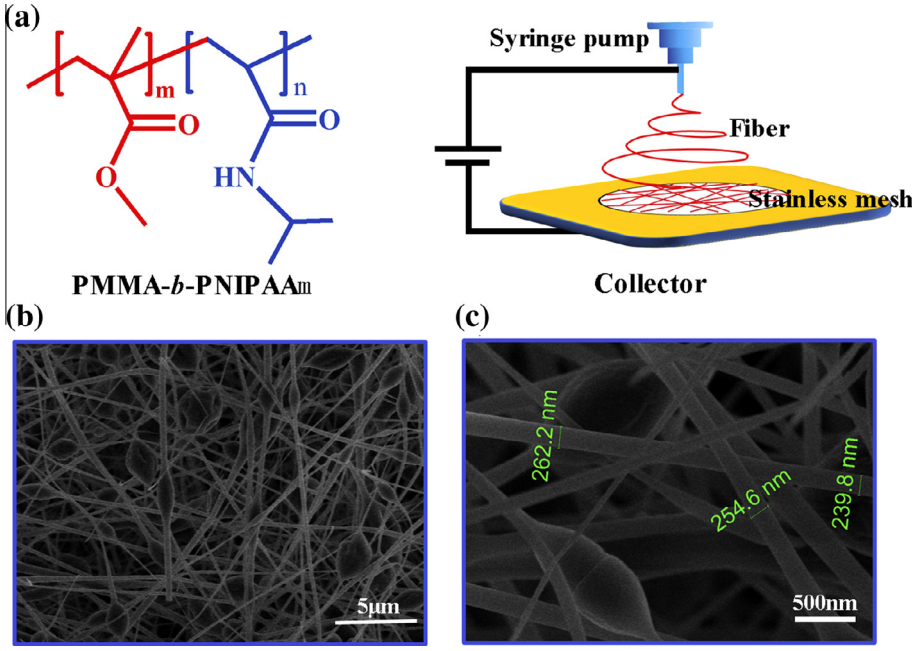

Fig. 2. (a) Diagram of the preparation process for electrospun fibrous membrane. (b and c) SEM images of a representative porous fibrous membrane with different magnifications.

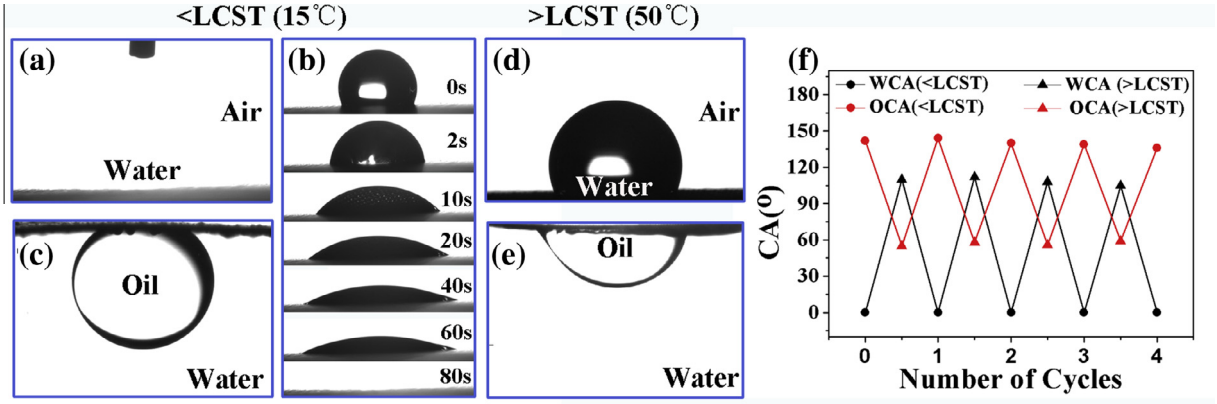

Fig. 3. Water and oil wettability of the solution-casting membrane at temperature below the LCST (a–c) and temperature above the LCST (d and e). (a) Image of a water droplet on the membrane in air with a water contact angle (WCA) of almost 0°. (b) Images of the dynamic water droplet spreading over the fiber membrane within 80 s. (c) Image of an oil droplet (hexane) on the membrane underwater with an oil contact angle (OCA) of ~142°. (d) Image of a water droplet on the membrane in air with a WCA of ~110°. (e) Image of an oil droplet (hexane) on the membrane underwater with an OCA of ~55°. (f) Reversible oil/water wettability at different temperatures.

capture, will effectively block the access of oil liquid, thus leading to the underwater oleophobic property of the membrane. In addition, according to the Wenzel's model [27], the increased surface roughness amplifies both water and oil wettability of the membrane. Consequently, the membrane with honeycomb surface morphology exhibits superhydrophilic and highly oleophobic properties. When the temperature increases above the LCST, PNIPAAm chains are dehydrated and collapsed because of the intramolecular hydrogen bonds between C=O and N—H groups. The membrane becomes hydrophobic in air. As to the oil wettability under water, the dehydration of PNIPAAm chains is improved by the incorporation of PMMA block. PNIPAAm domains become more oleophilic as water releases from the confined space. Meanwhile, the oil-favored PMMA also contribute to the oleophilic property of the membrane.

The water/oil wettability of the electrospun fibrous membrane was also characterized by the CA measurements at different temperatures. Below the LCST, the membrane exhibits superhydrophilic and underwater superoleophobic properties in Fig. 4a and c, respectively. It is worth noting that the water droplet spreading out the membrane in air only takes 12 s (Fig. 4b), which is a relatively short time compared with the water permeation time on the solution-casting membrane (80 s). As for oil wettability under water, hexane droplet on the membrane with OCA of about 153° can roll off the surface easily (Fig. 4c, right), which indicates that the membrane not only has superoleophobicity but also shows a quite low oil-adhesion property. Above the LCST, the wettability of the membrane switches to hydrophobicity and underwater oleophilicity. Water droplet with a WCA of about 130° can stably sit on the membrane in air (Fig. 4d) and hexane droplet on the surface in aqueous solution has an OCA of about 37° (Fig. 4e). These results indicate that the electrospun fibrous membrane has an enhanced temperature switchable oil/water wettability compared to the solution-casting membrane. Similarly, as seen in

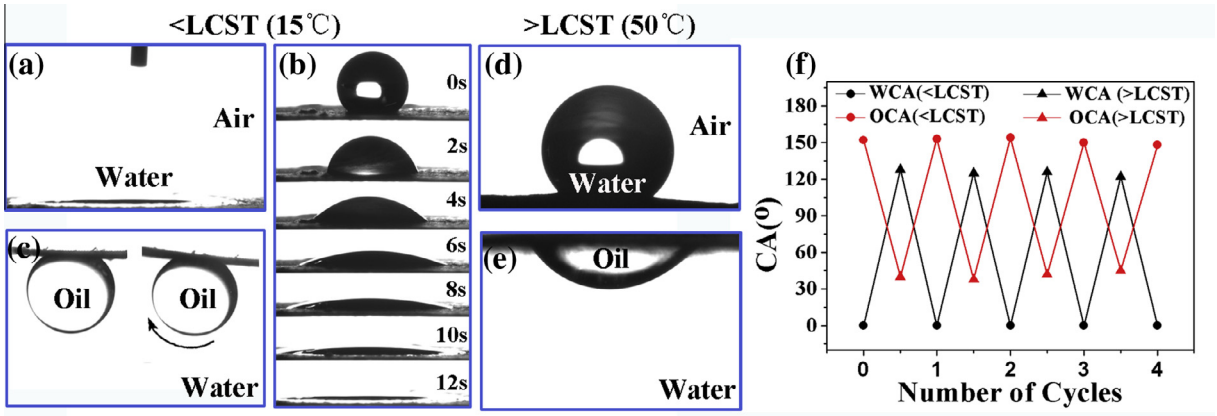

Fig. 4. Water and oil wettability of electrospun fibrous membrane at temperature below the LCST (a–c) and temperature above the LCST (d and e). (a) Image of a water droplet on the membrane in air with a WCA of almost 0°. (b) Images of the dynamic water droplet spread over the fiber membrane within 12 s. (c) Images of an oil droplet (hexane) on the membrane underwater with an OCA of ~153° (left) and sliding angle of ~4° (right). (d) Image of a water droplet on the membrane in air with a WCA of ~130°. (e) Image of an oil droplet (hexane) on the membrane underwater with an OCA of ~37°. (f) Reversible oil/water wettability at different temperatures.

Fig. 4f, the switching between wetting states of superhydrophili city/superoleophobicity and hydrophobicity/oleophilicity is also reversible.

As has been discussed above, the surface wettability can be influenced by the combination of chemical composition and surface morphology. Here, the temperature switchable oil/water wettability of the electrospun fibrous membrane is mainly attributed to the temperature responsiveness of the polymer, whereas the transition range of surface wettability is significantly extended by the 3D network porous structure of the fibrous membrane. More specifically, below the LCST, continuous nano-structured fibrous networks increase the surface roughness, leading to superhydrophilicity of the membrane. Meanwhile, the high porosity and large surface-to-volume ratio of the membrane effectively reduce the mass transfer resistance of the membrane and accelerate the permeation ratio of water. For oil wettability under water, the porous structure provides a plenty of pockets for retaining water. As water molecules with highly oil repellency are trapped in the pores of membrane, a barrier layer is formed and prevents the oil droplet contact with the surface. The membrane is hence endowed with superoleophobic and low oil-adhesive property. Above the LCST, the air trapped in the high-density micropores of membrane reduces the water contact area with membrane and contributes greatly to highly water repellency of the membrane. This explanation is consistent with the theory of Cassie–Baxter model [28]. In the case of underwater, air trapped in the surface also plays a crucial role in the oil affinity and water un-wetting performance. All in all, the responsiveness of PMMA-*b*-PNIPAAm and 3D network porous structure jointly enhance the temperature switchable oil/water wettability of the electrospun fibrous membrane.

3.3. Temperature controllable separation

Based on the temperature switchable oil/water wettability, both the as-prepared smart membranes are promising candidates for achieving controllable oil/water separations. Therefore, we carried out a series of proof-of-concept studies to test their controllable oil/water separation capacities. Typical separation procedure was performed as shown in Fig. 5. The smart membrane was fixed between two glass tubes with flanged connection and a beaker was placed at the bottom as the container (Fig. 5a). When a mixture of oil (n-hexane colored with ferrocene) and water was poured into the separation device, water selectively passed through the mesh (Fig. 5b) and was collected by the container (Fig. 5c), while oil was repelled and kept in the upper glass tube. After in situ heating the mesh using a 1100 W hair dryer for a certain time (Fig. 5d), oil started to permeate the mesh and the flow velocity increases gradually (Fig. 5e). The separation was accomplished and the oil was collected in another beaker (Fig. 5f).

In present work, the membrane was saturated by water prior to separation in order to ensure the success and efficiency of the separation. Detailed separation processes of solution-casting membrane and electrospun fibrous membrane were recorded in Supplementary movies SI1 and SI2, respectively. Separation efficiency and liquid flux were calculated to evaluate the separation performances of the two membranes obtained by different fabrication processes. Both membranes realized the separation of layered oil and water mixture by in situ adjusting the temperature and all the separation processes were driven solely by gravity. We calculated the separation efficiency of the membranes through comparing the weight of water before and after separation. Results summarized in Fig. 6a show that both membranes exhibit excellent separation efficiency higher than 99%. Then, water and oil fluxes of the membranes were obtained by calculating the permeation volume per unit time from the valid area (0.96×10^{-3} m^2). As shown in Fig. 6b, at the initial state, solution-casting membrane exhibits a water flux of about 6200 L h^{-1} m^{-2}, by contrast, electrospun fibrous membrane achieves a higher water flux of about 9400 L h^{-1} m^{-2}. After in situ heating the membrane in a certain time, oil began to permeate the membrane, and the speed gradually accelerated. Oil passed through the polymer solution-casting membrane with a flux of about 1550 L h^{-1} m^{-2}, in terms of the electrospun fibrous membrane, a promising oil flux of about 4200 L h^{-1} m^{-2} was obtained.

To better understanding the separation mechanism and separation performance, the microscopic structures and water/oil wetting states of the membranes during the separation process were modeled in Fig. 7. At initial state, the superhydrophilic membranes are wetted by water before separation, which facilitate water to pass through and oil to stay above the membrane (Fig. 7a). The electrospun fibrous membrane can be wetted in a short time, and water can go through it much quicker because of the high porosity and large surface-to-volume ratio of fibrous membrane. In addition, the stable underwater superoleophobic and ultralow oil-adhesive properties introduced by the continuous nano-structured fibrous networks will protect the membrane from being fouled by oil during separation, and make it exhibit an excellent oil-fouling repellency [29,30]. Subsequently, in situ heating the polymer membranes until the temperature above LCST, the wettability of membranes changes into hydrophobicity and oleophilicity. Water

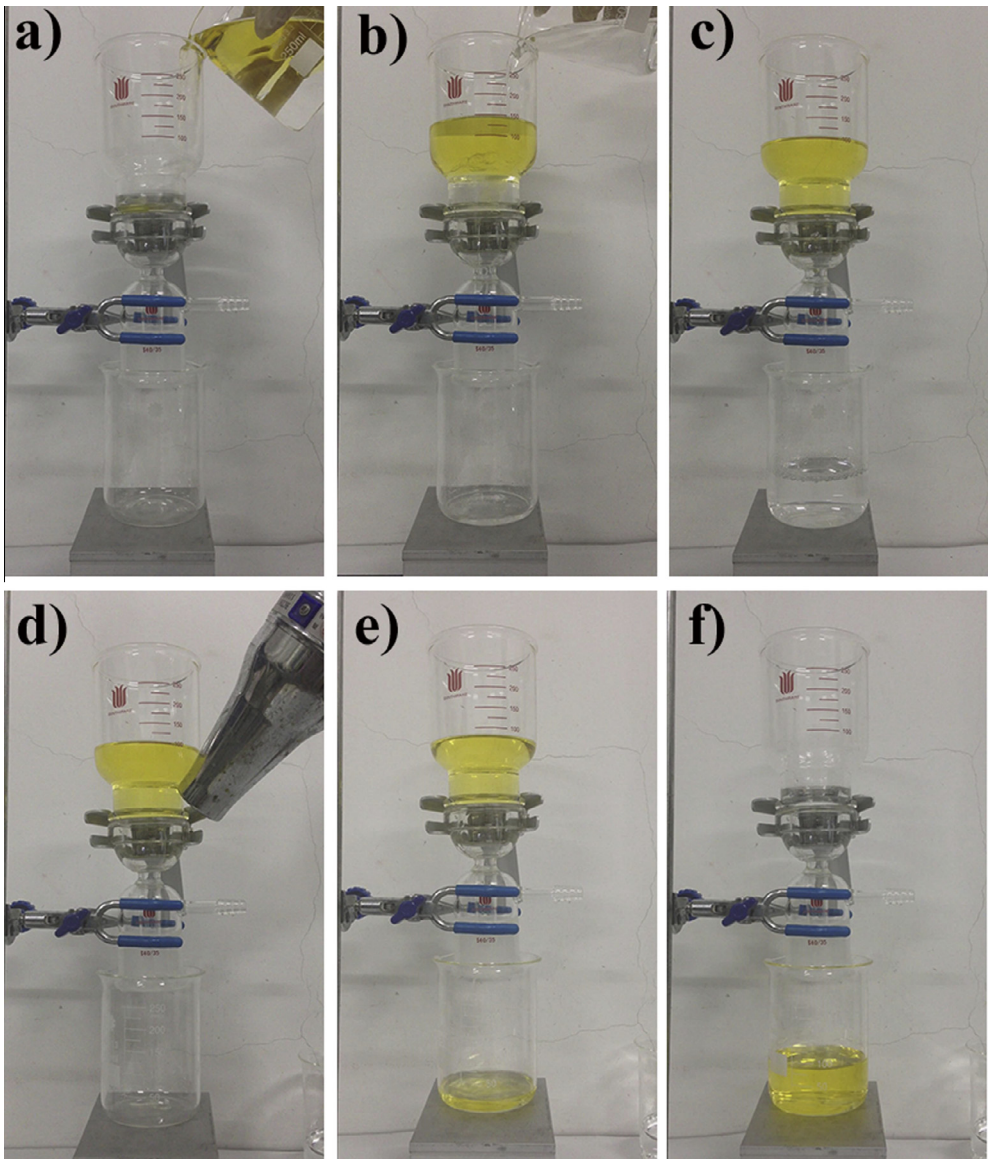

Fig. 5. Temperature controlled oil/water separation. (a) The as-prepared smart membrane was fixed between two glass tubes with flanged connection. A beaker was placed at the bottom as a container. (b) A mixture of water and oil (n-hexane colored with ferrocene) was poured into the upper glass tube. (c) Water passed through the membrane and was collected in a beaker, whereas the oil was remained in the upper glass tube. (d) The mesh was in situ heated by a hair dryer until block copolymer reached its LSCT. (e) The oil started to permeate the mesh and (f) was collected in another beaker. (For interpretation of the references to color in this figure legend, the reader is referred to the web version of this article.)

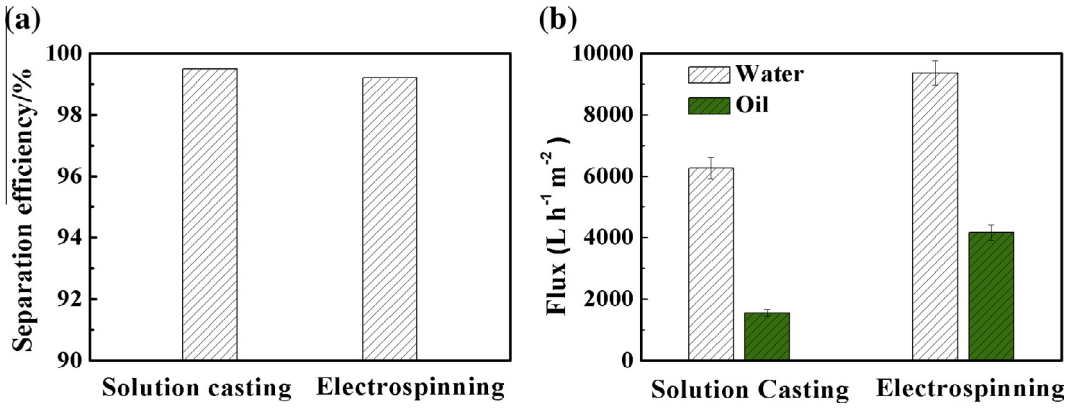

Fig. 6. Separation performances of membranes for oil (hexane) and water mixture. (a) Separation efficiency and (b) liquid (oil and water) fluxes of the membranes prepared by solution-casting method and electrospinning technology, respectively.

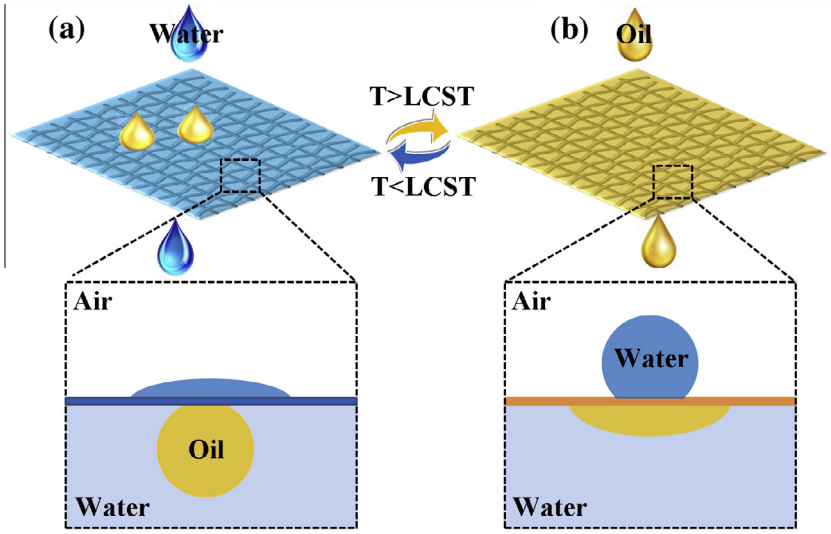

Fig. 7. (a) Schematic diagrams of temperature controlled oil/water separation. (a) At initial state, water goes through the membrane, whereas oil stays over the membrane. (b) After heating the membrane, oil passes through the membrane.

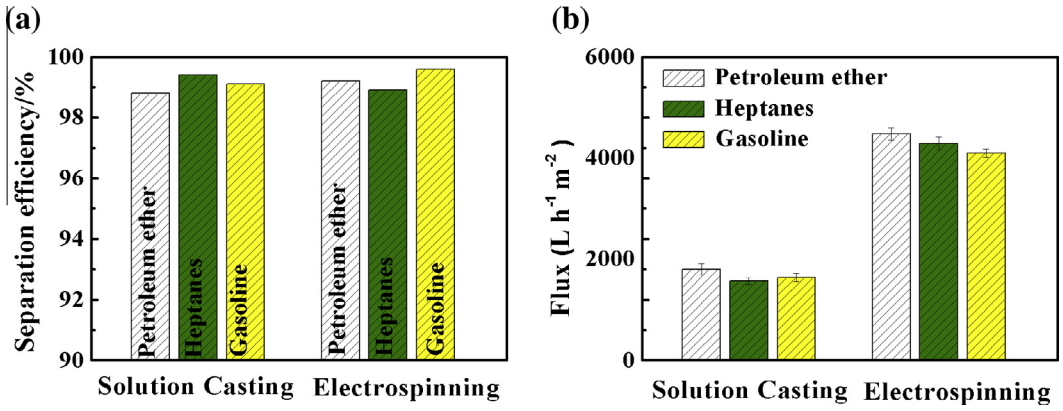

Fig. 8. Separation performances of membranes for different oil and water mixtures. (a) Separation efficiency and (b) oil fluxes of the membranes prepared by solution-casting method and electrospinning technology, respectively.

retained in the membranes is gradually replaced by the oil, and finally oil permeates through the membranes (Fig. 7b). Similarly, the higher porosity of the fibrous membranes is better for the formation of oil channel, leading to a higher oil flux. Therefore, characteristics of the high porosity and the large surface-to-volume ratio make the electrospun fibrous membrane exhibit a better separation performance than solution-casting membrane in terms of liquid flux.

In addition, the membranes exhibited similar temperature controllable separation behaviors for other oil types, such as petroleum ether, heptanes, and gasoline. Results in Fig. 8a show that both membranes achieve excellent separation efficiency higher than 98.5%. After in situ heating the membranes, the electrospun fibrous membrane obtains a higher oil flux (~4300 L h^{-1} m^{-2}) than the solution-casting membrane (~1600 L h^{-1} m^{-2}) (Fig. 8b). These promising separation performances demonstrate that electrospinning is a powerful and cost-effective method to construct smart membrane with randomly entangled fibers and high-density micropores. Such smart fibrous membrane with extended transition range of surface wettability can realize controllable oil/water separation with excellent performance, which is a good candidate for industrial oil spill cleanup and oil-polluted water disposal.

4. Conclusions

In summary, we constructed two PMMA-*b*-PNIPAAm based smart membranes with temperature-modulable oil/water wettability through solution-casting method and electrospinning technology, respectively. 3D network porous structure plays an important role in wetting behavior of electrospun fibrous membrane: randomly entangled fibers increase the roughness of membrane surface; high density micropores further improve the wetting and anti-wetting property of the membrane. Therefore, the electrospun fibrous membrane owned an extended transition range of oil/water wettability compared to the solution-casting membrane. At last, the as-prepared membranes realized the gravity-driven oil/water separation with efficiency higher than 98.5% through regulating temperature. Solution-casting membrane exhibited a water flux of about 6200 L h^{-1} m^{-2} and an oil flux of about 1550 L h^{-1} m^{-2}. By contrast, characteristics of the high porosity and the large surface-to-volume ratio made the electrospun fibrous membrane achieve higher fluxes of about 9400 L h^{-1} m^{-2} for water and 4200 L h^{-1} for oil. On the basis of this understanding, we believe that electrospinning is a powerful and cost-effective method, which can be employed to construct smart membrane with special surface morphology and excellent

switchable wetting behavior. The membrane holds promise in myriad applications including wastewater treatment, biomedicine, microfluidic devices and nanoreactors.

Acknowledgments

The authors thank the National Natural Science Foundation of China (No. 21276213), the Research Fund for the Doctoral Program of Higher Education (No. 20130073110077) and the National High Technology Research and Development Program of China (No. 2013AA032302) for supporting this work.

Appendix A. Supplementary data

Supplementary data associated with this article can be found, in the online version, at http://dx.doi.org/10.1016/j.cej.2015.11.057.

References

[1] M.A. Shannon, P.W. Bohn, M. Elimelech, J.G. Georgiadis, B.J. Marinas, A.M. Mayes, Science and technology for water purification in the coming decades, Nature 452 (2008) 301–310.
[2] D.D. Nguyen, N.-H. Tai, S.-B. Lee, W.-S. Kuo, Superhydrophobic and superoleophilic properties of graphene-based sponges fabricated using a facile dip coating method, Energy Environ. Sci. 5 (2012) 7908–7912.
[3] Z.L. Chu, Y.J. Feng, S. Seeger, Oil/water separation with selective superantiwetting/superwetting surface materials, Angew. Chem. Int. Ed. 54 (2015) 2328–2338.
[4] L.B. Zhang, Z.H. Zhang, P. Wang, Smart surfaces with switchable superoleophilicity and superoleophobicity in aqueous media: toward controllable oil/water separation, NPG Asia Mater. 4 (2012) e8.
[5] B.L. Xue, L.C. Gao, Y.P. Hou, Z.W. Liu, L. Jiang, Temperature controlled water/oil wettability of a surface fabricated by a block copolymer: application as a dual water/oil on–off switch, Adv. Mater. 25 (2013) 273–277.
[6] Y.Z. Cao, N. Liu, C.K. Fu, K. Li, L. Tao, L. Feng, Y. Wei, Thermo and pH dual-responsive materials for controllable oil/water separation, ACS Appl. Mater. Interfaces 6 (2014) 2026–2030.
[7] Y.-N. Zhou, J.-J. Li, Q. Zhang, Z.-H. Luo, Light-responsive smart surface with controllable wettability and excellent stability, Langmuir 30 (2014) 12236–12242.
[8] G. Kwon, A. Kota, Y.X. Li, A. Sohani, J.M. Mabry, A. Tuteja, On-demand separation of oil–water mixtures, Adv. Mater. 24 (2012) 3666–3671.
[9] Z.X. Xue, M.J. Liu, Lei Jiang, Recent developments in polymeric superoleophobic surfaces, J. Polym. Sci. Part B: Polym. Phys. 50 (2012) 1209–1224.
[10] B. Wang, W. Liang, Z. Guo, W. Liu, Biomimetic super-lyophobic and super-lyophilic materials applied for oil/water separation: a new strategy beyond nature, Chem. Soc. Rev. 44 (2015) 336–361.
[11] S. Schmidt, H. Motschmann, T. Hellweg, R. von Klitzing, Thermoresponsive surfaces by spin-coating of PNIPAM-co-PAA microgels: a combined AFM and ellipsometry study, Polymer 49 (2008) 749–756.
[12] Y.-N. Zhou, J.-J. Li, Z.-H. Luo, PhotoATRP-based fluorinated thermo-sensitive block copolymer for controllable water/oil separation, Ind. Eng. Chem. Res. 54 (2015) 10714–10722.
[13] H. Wang, Y. Xue, T. Lin, One-step vapour-phase formation of patternable, electrically conductive, superamphiphobic coatings on fibrous materials, Soft Matter 7 (2011) 8158–8161.
[14] H. Che, M. Huo, L. Peng, T. Fang, N. Liu, L. Feng, Y. Wei, J. Yuan, CO_2-responsive nanofibrous membranes with switchable oil/water wettability, Angew. Chem. Int. Ed. 54 (2015) 8934–8938.
[15] J. Borges, L.C. Rodrigues, R.L. Reis, J.F. Mano, Layer-by-layer assembly of light-responsive polymeric multilayer systems, Adv. Funct. Mater. 24 (2014) 5624–5648.
[16] J.-J. Li, Y.-N. Zhou, Z.-H. Luo, Smart fiber membrane for pH-induced oil/water separation, ACS Appl. Mater. Interfaces 7 (2015) 19643–19650.
[17] X. Wang, B. Ding, G. Sun, M. Wang, J. Yu, Electro-spinning/netting: a strategy for the fabrication of three-dimensional polymer nano-fiber/nets, Prog. Mater. Sci. 58 (2013) 1173–1243.
[18] V. Percec, T. Guliashvili, J.S. Ladislaw, A. Wistrand, A. Stjerndahl, M.J. Sienkowska, M.J. Monteiro, S. Sahoo, Ultrafast synthesis of ultrahigh molar mass polymers by metal-catalyzed living radical polymerization of acrylates, methacrylates, and vinyl chloride mediated by SET at 25 °C, J. Am. Chem. Soc. 128 (2006) 14156–14165.
[19] Y.-N. Zhou, Z.-H. Luo, Copper (0)-mediated reversible-deactivation radical polymerization: kinetics insight and experimental study, Macromolecules 47 (2014) 6218–6229.
[20] J.-J. Li, Y.-N. Zhou, Z.-H. Luo, Thermal-responsive block copolymers for surface with reversible switchable wettability, Ind. Eng. Chem. Res. 53 (2014) 18112–18120.
[21] S.L. Hsu, Poly(methyl methacrylate), in: J.E. Mark (Ed.), Polymer Data Handbook, Oxford Press, New York, 1999, p. 656.
[22] N.A. Peppas, Poly(N-isopropyl acrylamide), in: J.E. Mark (Ed.), Polymer Data Handbook, Oxford Press, New York, 1999, p. 625.
[23] T.L. Sun, G.J. Wang, L. Feng, B.Q. Liu, Y.M. Ma, L. Jiang, D.B. Zhu, Reversible switching between superhydrophilicity and superhydrophobicity, Angew. Chem. Int. Ed. 43 (2004) 357–360.
[24] L. Chen, M. Liu, L. Lin, T. Zhang, J. Ma, Y. Song, L. Jiang, Thermal-responsive hydrogel surface: tunable wettability and adhesion to oil at the water/solid interface, Soft Matter 6 (2010) 2708–2712.
[25] M. Liu, S. Wang, Z. Wei, Y. Song, L. Jiang, Bioinspired design of a superoleophobic and low adhesive water/solid interface, Adv. Mater. 21 (2009) 665–669.
[26] A. Tuteja, W. Choi, M. Ma, J.M. Mabry, S.A. Mazzella, G.C. Rutledge, G.H. McKinley, R.E. Cohen, Designing superoleophobic surfaces, Science 318 (2007) 1618–1622.
[27] R.N. Wenzel, Resistance of solid surfaces to wetting by water, Ind. Eng. Chem. 28 (1936) 988–994.
[28] A.B.D. Cassie, S. Baxter, Wettability of porous surfaces, Trans. Faraday Soc. 40 (1944) 546–551.
[29] X. Zheng, Z.Y. Guo, D.L. Tian, X.F. Zhang, W.X. Li, L. Jiang, Underwater self-cleaning scaly fabric membrane for oily water separation, ACS Appl. Mater. Interfaces 7 (2015) 4336–4343.
[30] Y.Z. Zhu, W. Xie, J.Y. Li, T.L. Xing, J. Jin, pH-Induced non-fouling membrane for effective separation of oil-in-water emulsion, J. Membr. Sci. 477 (2015) 131–138.